

Syntheses, Structure and Photoluminescence Properties of Silver(I) Complexes with Naphthalene Iminoimides

Hong Yang,^[a] Yan-Ni Lao,^[a] Jia-Min Chen,^[a] Hui-Xia Wu,^[a] and Shi-Ping Yang*^[a]

Keywords: Silver / N ligands / Luminescence / Structure elucidation / Metal–organic frameworks

Three silver(I) complexes, namely $[\text{Ag}(\text{L})(\text{NO}_3)]_\infty$ (**1**), $[\text{Ag}(\text{L})_2(\text{NO}_3)]$ (**2**) and $[\text{Ag}(\text{L})_2(\text{BF}_4)]$ (**3**) [$\text{L} = 9,10\text{-dihydro-7H-benzo-}[\text{de}]\text{imidazo}[2,1-a]\text{isoquinolin-7-one}$], have been synthesized and characterized by X-ray crystallography, elemental analyses and FTIR spectra. The counteranions in the Ag^{I} salts and the ligand/ Ag^{I} ratio play fundamental roles in the formation of Ag^{I} complexes having different crystal structures. The Ag^{I} ions in **1** and **2** are both three-coordinate, but they are two-coordinate in **3**. Complex **1** adopts the polymeric chain-like structure mainly bridged by nitrate anions. These chains are assembled into 2D sheets by the π – π stacking interaction of the ligands between the adjacent chains and weak intermolecular hydrogen bonds. They are further packed into 3D

networks by C–H...O hydrogen bonds. For **2** and **3**, mononuclear silver(I) complexes are formed. Complex **2** is extended into an infinite zigzag chain with knots by the π – π stacking interactions of the ligands and further assembled by C–H...O interactions. However, the tetrafluoroborate anions in **3** are not coordinated but are connected by intermolecular hydrogen bonds to form an infinite molecular ladder with ligand-supported Ag–N inner rungs. All the complexes display room-temperature photoluminescence in the visible region, which may be assigned to ligand-centred π – π^* transitions supported by the theory calculation.

(© Wiley-VCH Verlag GmbH & Co. KGaA, 69451 Weinheim, Germany, 2009)

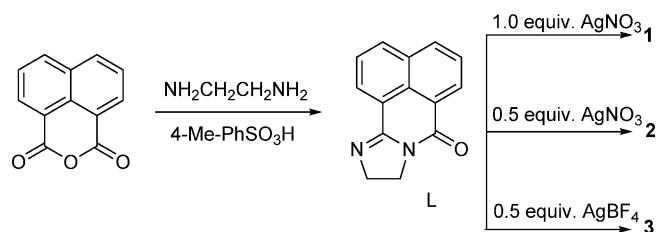
Introduction

Great interest has recently been focused on the crystal engineering of novel coordination polymers, not only due to their fascinating structures but also due to their potential applications as functional materials.^[1] In recent years, luminescent metal complexes have been extensively studied. Among these, d^{10} complexes exhibit rich luminescent properties due to the versatility of excited states such as ligand-centred, charge-transfer or, in the case of polynuclear compounds, even metal-centred transitions.^[2] In some cases, coordination polymers have more advantages in controlling emission properties in comparison with organic complexes.

The Ag^{I} ion is regarded as a soft acid that favours the coordination of soft bases, such as ligands that contain sulfur and unsaturated nitrogen.^[3] Although the influences on coordination polymers are not yet well understood, silver(I) coordination architectures have been documented to be heavily influenced by various factors such as the coordination geometry, counteranion, metal-to-ligand ratio,^[4] solvent effects and reaction conditions,^[5] as well as the nature of the ligand.^[6]

Ligands containing imidazole groups have attracted considerable interest for their wide-ranging properties and ver-

satile coordination modes. Many silver(I) complexes with imidazole and its derivatives as ligands are also considered as useful models to study metal–ligand interactions, in which different kinds of the mononuclear,^[7] dinuclear^[8] and polynuclear^[9] silver(I) complexes with a variety of coordination geometries are involved. We are currently investigating the formation of novel coordination polymers obtained through the interaction between transition-metal ions and different ligands containing the imidazole group^[10] and are planning to design new imidazole-containing ligands by introducing large conjugated segments. 1,8-naphthalimide derivatives are good candidates because of their intrinsic photophysical and photochemical properties,^[11] which are well known in their use as fluorescent dyes^[12] and fluorescent markers.^[13] On the basis of the above-mentioned considerations, in this study, 9,10-dihydro-7H-benzo[de]imidazo[2,1-a]isoquinolin-7-one (**L**, see Scheme 1) was synthesized by the condensation of 1,8-naphthalic anhydride and ethylenediamine by following the reported method.^[14] Three Ag^{I} com-



Scheme 1. Synthesis route of the ligand and complexes.

[a] Department of Chemistry, College of Life and Environmental Science, Shanghai Normal University, Shanghai 200234, P. R. China
Fax: +86-21-64322511
E-mail: shipingyang@shnu.edu.cn

Supporting information for this article is available on the WWW under <http://dx.doi.org/10.1002/ejic.200900242>.

plexes, namely, $[\text{Ag}(\text{L})(\text{NO}_3)]_\infty$ (**1**), $[\text{Ag}(\text{L})_2(\text{NO}_3)]$ (**2**) and $[\text{Ag}(\text{L})_2(\text{BF}_4)]$ (**3**), were obtained and characterized (Scheme 1). Emission spectra of these complexes and of the ligand were also measured to explore the relationship with their packing interactions in different coordination geometries.

Results and Discussion

Syntheses and General Characterization

L was prepared in approximately 90% yield as a yellow solid by the reaction of 1,8-naphthalic anhydride and ethylenediamine, and it was characterized by ^1H NMR and FTIR spectroscopy.^[15] Three silver(I) complexes with the different metal–ligand ratios were obtained with AgNO_3 and AgBF_4 . The elemental analysis data are in agreement with those of the target products. All the complexes are air-stable at room temperature.

The characteristic feature of the FTIR spectra of **1–3** is the strong absorption around 1615 cm^{-1} , which corresponds to the stretching vibrations of $\text{C}=\text{N}$ groups. These relatively lower frequencies for the $\text{C}=\text{N}$ groups with respect to those of the ligand (1645 cm^{-1}) suggest that the nitrogen atoms of the $\text{C}=\text{N}$ groups in the imidazole ring participate in the

coordination, which is confirmed by X-ray crystallography. The absorption band around 1380 cm^{-1} indicates the presence of coordinated and dissociative nitrate anions in **1** and **2**. In **3**, the characteristic band appearing at 1055 cm^{-1} indicates the existence of the BF_4^- anion. Furthermore, the FTIR spectra of **1–3** also show the expected medium-to-weak absorption bands in the range $1550\text{--}1600\text{ cm}^{-1}$ due to the breathing of the naphthyl rings.

Crystal Structure

$[\text{Ag}(\text{L})(\text{NO}_3)]_\infty$ (**1**)

X-ray diffraction analysis shows that **1** has an infinite polymeric 1D chain structure, and all the Ag^{I} centres, **L** and the nitrate anions in **1** are equivalent (see Figure 1a). Interestingly, each Ag^{I} ion is linked to two O atoms from different nitrate anions [$\text{Ag}^{\text{I}}\text{--O}(2)$ $2.378(4)\text{ \AA}$ and $\text{Ag}^{\text{I}}\text{--O}(3)$ $2.498(5)\text{ \AA}$] and an N atom of **L** [$\text{Ag}^{\text{I}}\text{--N}$ $2.186(4)\text{ \AA}$] in a triangular fashion with a nonbonding $\text{Ag}\cdots\text{Ag}$ distance of 5.302 \AA connected by nitrate anions. The sum (357.9°) of the angles N--Ag--O [$142.28(13)^\circ$ and $127.04(13)^\circ$] and O--Ag--O [$88.6(1)^\circ$] confirms a nearly planar environment around each Ag^{I} centre. It should be pointed out that two adjacent ligand rings in the chain are all in a staggered fash-

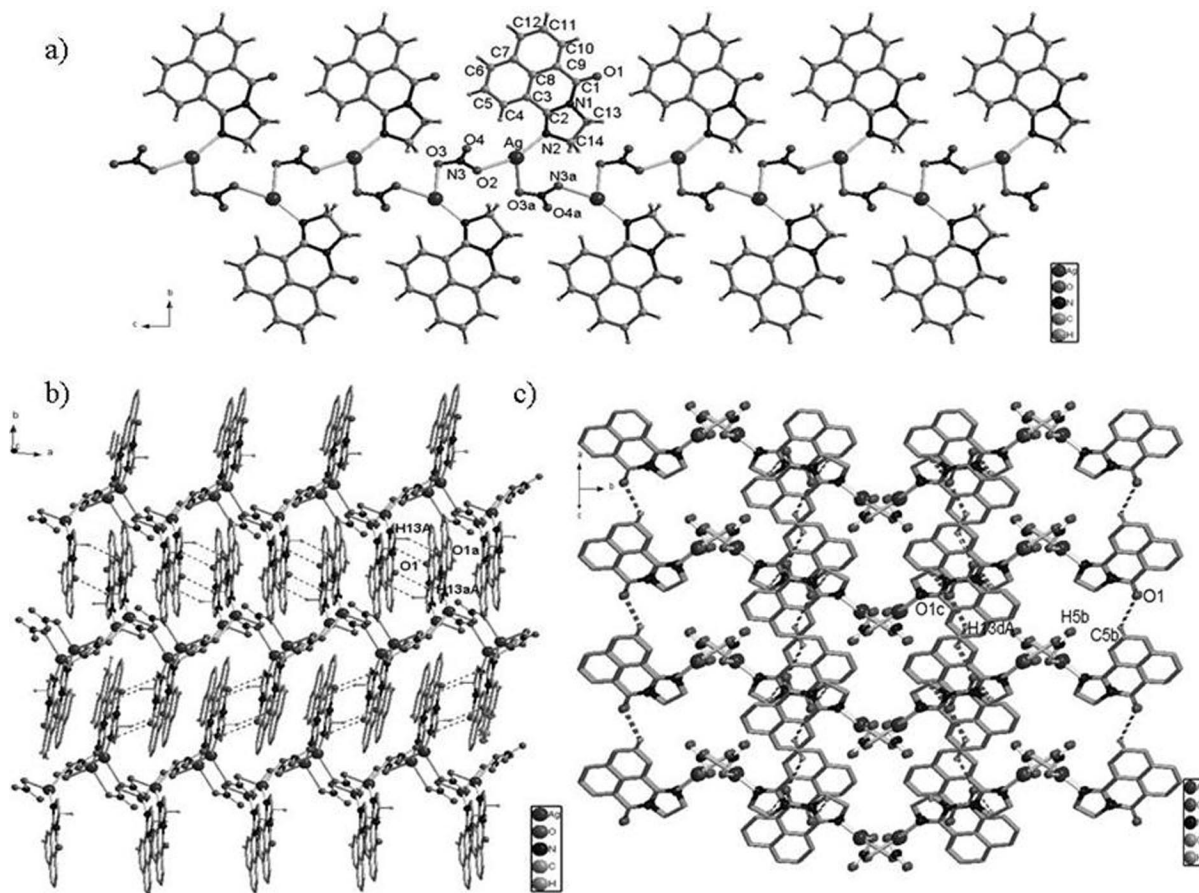


Figure 1. View of (a) the 1D polymeric chain, (b) the 2D sheet and (c) the 3D supramolecular networks in **1** (H atoms omitted for clarity). Symmetry codes are a: $1 + x, 1 + y, -1 + z$; A: $0.5 + x, 0.5 - y, 1.5 + z$; b: $-1 - x, 1 - y, -z$; c: $-1.5 + x, 0.5 - y, -2.5 + z$.

ion, no significant π - π stacking interaction is thus found. In contrast, weak C-H \cdots O hydrogen bonds and π - π interactions are observed between adjacent chains. The distance of C(4) \cdots O(4) is 3.344(7) Å, and the angle C(4)-H(4) \cdots O(4) is 146°. The ligand rings are approximately parallel to each other with a dihedral angle of 7.7° and face-to-face alternate distances of 3.3786(2) and 3.3623(4) Å, indicating significant π - π stacking interactions between the adjacent ligand rings. The chains are further assembled by weak C-H \cdots O hydrogen bonds and π - π interactions between adjacent chains into an infinite 2D supramolecular sheet (Figure 1b). Additionally, there are also weak C-H \cdots O hydrogen bonds between the 2D sheets (Tables 1 and 2). Thus,

Table 1. Selected hydrogen bonds for 1–3.

D-H \cdots A	D-H [Å]	H \cdots A [Å]	D \cdots A [Å]	D-H \cdots A [°]
1				
C(4)-H(4) \cdots O(4)	0.93	2.53	3.344(7)	146
C(5)-H(5) \cdots O(1)i	0.93	2.46	3.156(6)	132
C(13)-H(13A) \cdots O(1)ii	0.97	2.44	3.284(6)	145
C(14)-H(14B) \cdots O(2)iii	0.97	2.60	3.259(6)	126
2				
C(12)-H(12) \cdots O(3)j	0.93	2.47	3.190(5)	135
C(13)-H(13A) \cdots O(5)ii	0.97	2.53	3.381(6)	146
C(13)-H(13B) \cdots O(1)iii	0.97	2.55	3.335(5)	138
C(14)-H(14A) \cdots O(4)	0.97	2.45	3.157(7)	130
C(19)-H(19) \cdots O(2)iv	0.93	2.43	3.157(5)	135
C(27)-H(27A) \cdots O(2)v	0.97	2.59	3.483(5)	154
C(28)-H(28B) \cdots O(5)vi	0.97	2.31	3.248(7)	163
3				
C(5)-H(5) \cdots O(1) i	0.93	2.50	3.188 (6)	131
C(12)-H(12) \cdots F(2)ii	0.93	2.46	3.37(2)	168
C(13)-H(13A) \cdots O(1)iii	0.97	2.56	3.380(5)	142

the 2D sheets are further extended into 3D square grid supramolecular networks by the weak C-H \cdots O hydrogen bonds (Figure 1c).

Table 2. Selected bond lengths [Å] and angles [°] for 1–3.

1			
Ag–N(2)	2.186(4)	N(2)–Ag–O(2)	142.3(1)
Ag–O(3)	2.498(5)	O(2)–Ag–O(3)	88.6(1)
Ag–O(2)	2.378(4)	N(2)–Ag–O(3)	127.0(1)
2			
Ag–N(4)	2.136(3)	N(4)–Ag–N(2)	165.4(1)
Ag–N(2)	2.143(3)	N(4)–Ag–O(3)	94.8(1)
		N(2)–Ag–O(3)	99.7(1)
3			
Ag–N(1)	2.093(3)	N(1)–Ag–N(1a)	180.0

[Ag(L)₂(NO₃)] (2)

In comparison with **1**, complex **2** exhibits an obviously different conformation and features a mononuclear silver(I) complex (Figure 2a). The unique Ag^I centre is linked to two nitrogen donors of two different ligands [Ag–N lengths being 2.136(3) and 2.143(3) Å] and also to one oxygen atom of a nitrate anion by a weak Ag \cdots O [2.736(4) Å] interaction, which is not similar to that in **1**, resulting in an approximately T-shaped mononuclear unit. The Ag centre adopts a triangular configuration. The sum (359.92°) of the angles N–Ag–N [165.41(12)°] and N–Ag–O [94.82(12)° and 99.69(12)°] confirms a nearly planar coordination environment around each Ag^I centre, which is similar to that in **1**.

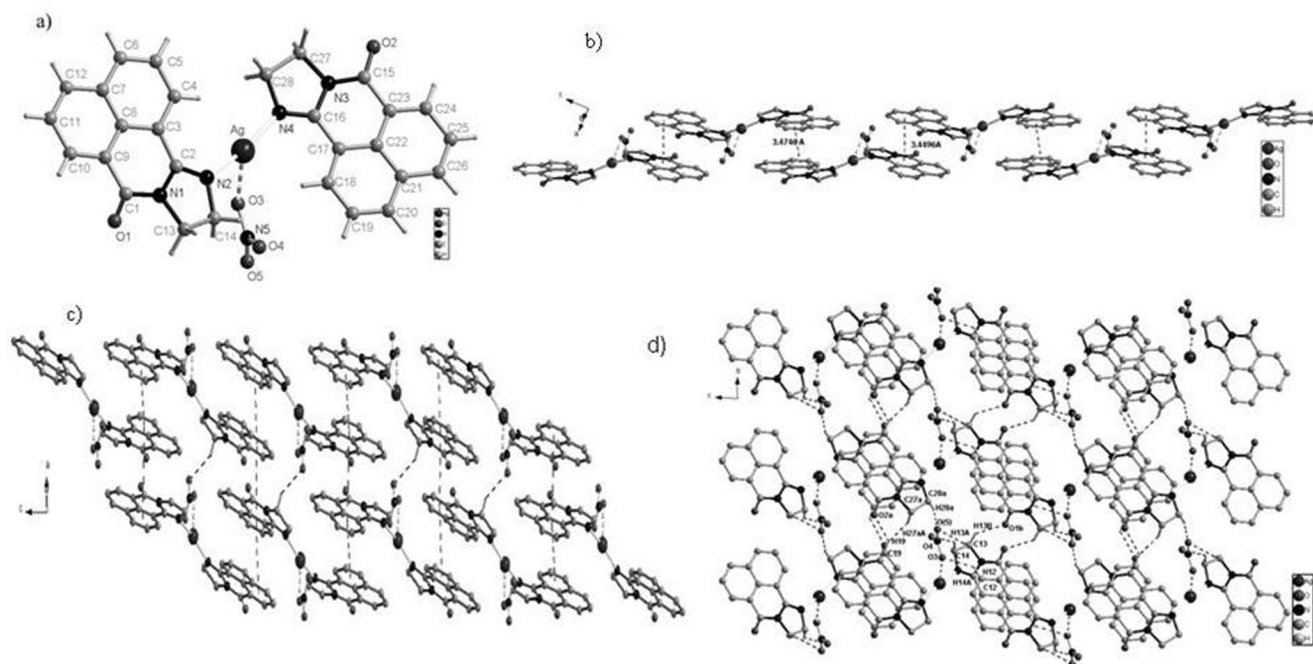


Figure 2. (a) Perspective view, (b) the 1D chain, (c) the 2D sheet and (d) the 3D supramolecular networks in **2** (H atoms omitted for clarity). Symmetry code a: 1 + x, y, z.

The ligand naphthyl rings are approximately parallel to each other with a dihedral angle of 9.3° . The Ag–O bond is longer than that in **1**, while the Ag–N bond lengths in **1** and **2** are nearly equal. More interestingly, the mononuclear units are connected by strong $\pi \cdots \pi$ stacking interactions of the naphthyl segment with a centroid–centroid separation of 3.478 \AA to form an infinite zigzag chain with knots (Figure 2b). Weak C–H \cdots O hydrogen bonds between O atoms from the nitrate anion and H atoms from ligand L are observed between adjacent chains. The distance C(28) \cdots O(5) is $3.248(7) \text{ \AA}$, and the angle C(28)–H(28B) \cdots O(5)^{vi} is 163° (Symmetry code: ^{vi} $x, -1 + y, z$). The chains are further assembled by the weak C–H \cdots O hydrogen bonds into an infinite 2D supramolecular sheet (Figure 2c). In addition, weak C–H \cdots O hydrogen bonds are observed between adjacent chains. The distances C(12) \cdots O(3)ⁱ, C(13) \cdots O(5)ⁱⁱ, C(13) \cdots O(1)ⁱⁱⁱ, C(14) \cdots O(4), C(19) \cdots O(2)^{iv} and C(27) \cdots O(2)^v are $3.190(5)$, $3.381(6)$, $3.335(5)$, $3.157(7)$, $3.157(5)$ and $3.483(5) \text{ \AA}$, respectively, and the angles C(12)–H(12) \cdots O(3)ⁱ, C(13)–H(13A) \cdots O(5)ⁱⁱ, C(13)–H(13B) \cdots O(1)ⁱⁱⁱ, C(14)–H(14A) \cdots O(4), C(19)–H(19) \cdots O(2)^{iv} and C(27)–H(27A) \cdots O(2)^v are 135 , 146 , 138 , 130 , 135 and 154° , respectively (Symmetry codes: ⁱ $-x, -y, 1 - z$; ⁱⁱ $-1 + x, y, z$; ⁱⁱⁱ $-1 - x, 1 - y, 1 - z$; ^{iv} $1 + x, 1 + y, z$; ^v $1 - x, -1 - y, 2 - z$). Similarly to **1**, the 2D sheets are further extended into 3D square grid supramolecular networks by these weak C–H \cdots O hydrogen bonds (Figure 2d).

[Ag(L)₂](BF₄) (**3**)

The Z-shaped mononuclear structure of **3** is distinct from those of **1** and **2**: the Ag^I ion is coordinated by two nitrogen atoms from two different naphthalene iminoimide ligands, exhibiting a linear geometry with a N(1)–Ag(1)–N(1) angle of 180° (Figure 3a). The Ag–N bond lengths [$2.093(3) \text{ \AA}$] are shorter than those in **2** [$2.143(3) \text{ \AA}$] and **1** [$2.186(4) \text{ \AA}$], but they fall in the normal range for other two-coordinate Ag^I complexes.^[16] It is noteworthy that all ligands are equivalent and are completely parallel to each other. It is interesting that in **3**, the mononuclear unit is connected by intermolecular hydrogen bonds [C(5) \cdots O(1) $3.188(6) \text{ \AA}$] (Figure 3b), and both ligands bridge Ag atoms through Ag–N bonds as inner rungs, resulting in an infinite molecular ladder. In the *ac* plane, the sides of adjacent ladders are connected by weak C \cdots F hydrogen bonds [C(13) \cdots F(2) $3.37(2) \text{ \AA}$] into an infinite 2D supramolecular sheet (Figure 3c). There are strong π – π stacking interactions between naphthalene iminoimide ligands, with a centroid–centroid separation of 3.481 \AA , and weak C–H \cdots O hydrogen bonds [C(13) \cdots O(1)ⁱⁱⁱ $3.284(6) \text{ \AA}$, C(13)–H(13A) \cdots O(1)ⁱⁱⁱ 145°] between adjacent 2D sheets,^[17] which results in square grid supramolecular networks.

The role of the counteranion is evident when we compare the reactivity of L with AgNO₃ and AgBF₄ in the 1:1 and 1:2 metal/ligand molar ratios. The presence of a small and

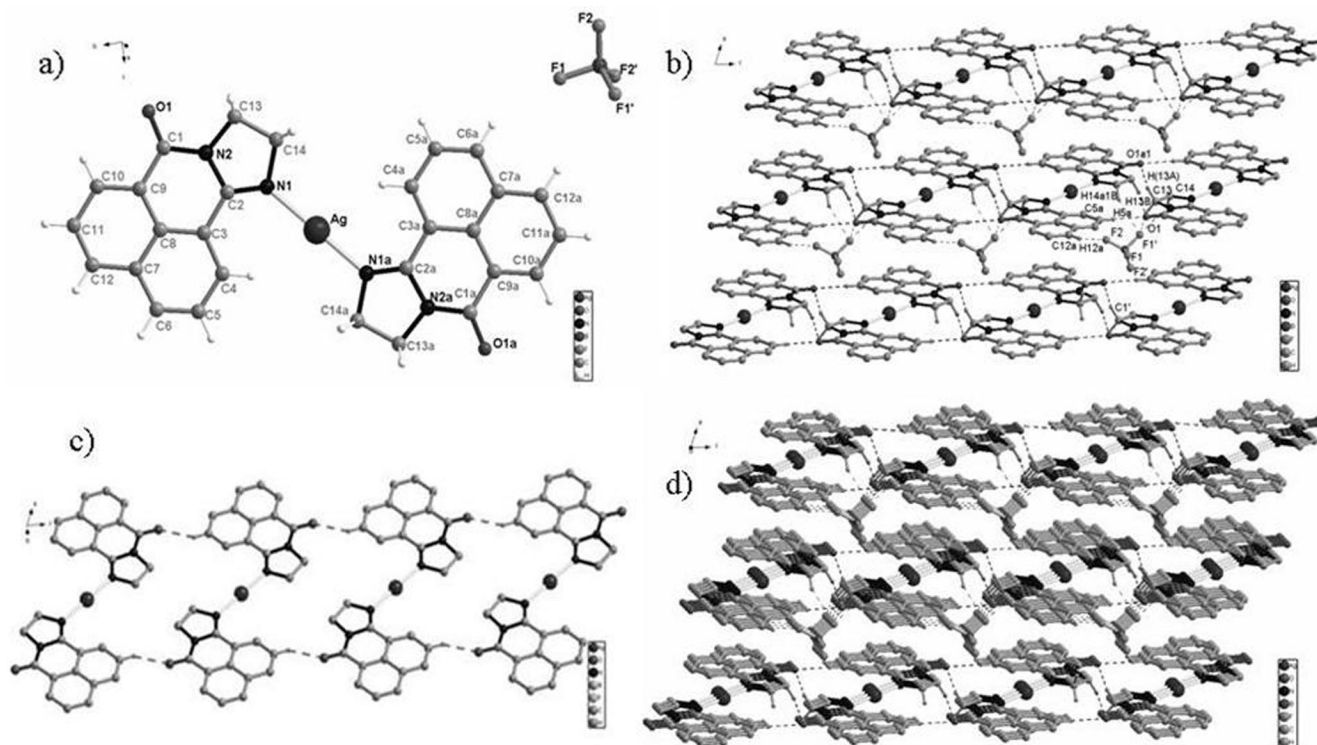
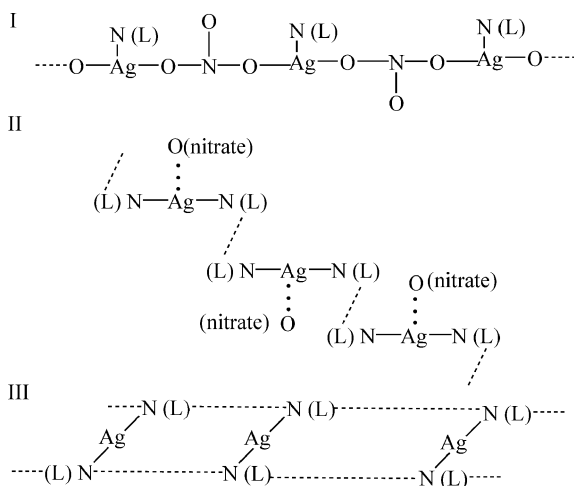


Figure 3. (a) Perspective view, (b) the 1D chain, (c) the 2D sheet and (d) the 3D diagram in **3**. Symmetry codes are a: $x, y, 1 + z$; A: $x, 1 + y, 1 + z$; B: $2 - x, 2 + y, 2 - z$.

moderate coordinating anion (NO_3^-) leaves the possibility of the formation of both the 1:1 and 1:2 complexes, while in the case of the tetrafluoroborate salt only the 1:2 species are obtained despite the metal/ligand ratio used. The weakly coordinating tetrafluoroborate anions have no significant influence in the coordination of the Ag^{I} ion even at increased metal/ligand molar ratios. This effect is basically attributable to the nature of the counteranion.^[4a]

Thermogravimetric Analysis

Thermogravimetric analysis (TGA) for **1–3** was performed from 26 to 800 °C in air, and the TGA curves are provided in Figures S1–S3. The results show that **1** decomposes at 187 °C, and **2** and **3** decompose at 268 and 246 °C, respectively, which indicates that the three complexes have high thermal stability. The difference in decomposition temperature between **1**, **2** and **3** may be attributed to the different association patterns of the Ag^I centres through the ligands into the supramolecular network structures described above. Scheme 2 illustrates the diagram of coordination patterns in the compounds. Complex **1** adopts mode I, and Ag–O bonds, being longer than Ag–N bonds, play an important role, which leads to the relatively lower decomposition temperature. Complexes **2** and **3** are best described by modes II and III, respectively. The isolated monomer structure is observed in **2** and **3**, and then the discrete association is adopted into an infinite structure. These structural features explain the higher temperatures of decomposition.



Scheme 2.

Luminescent Properties

The room-temperature luminescence spectra of the ligand and the three complexes are illustrated in Figure 4. When excited at 365 nm, compounds **1**, **2** and **3** exhibit fluorescence emission bands at 477, 497 and 500 nm, respectively. Compared with the fluorescence emission band of the ligand at 518 nm, the bands of **1–3** display a blueshift

with slightly different band shapes. Although these complexes contain silver(I) centres coordinated by the ligand, the Ag...Ag separations (5.302 Å in **1**, 8.724 Å in **2**, 9.301 Å in **3**) are much longer than the upper limit of 3.30 Å for ligand-to-metal-charge-transfer (LMCT).^[18] Consequently, the cluster-centred emission often accompanying the ligand-to-metal-charge-transfer (LMCT) excited state due to metal-metal bonding is not favoured in these complexes. Therefore, the emissions may be assigned to ligand-centred $\pi-\pi^*$ transitions. Similar assignments have also been reported for a luminescent Ag^I complex.^[2,19] The difference in the emission bands of these silver(I) complexes are mainly attributable to the intensity of intermolecular $\pi-\pi$ interactions of naphthalene iminoimide ligand in the solid state. According to the energy-gap law for radiationless deactivation,^[20] the luminescence of **1–3** should be redshifted relative to that of the corresponding ligand. However, the results in this study are not in accordance with this law (Figure 4), and the same phenomenon was also reported in the literature.^[21]

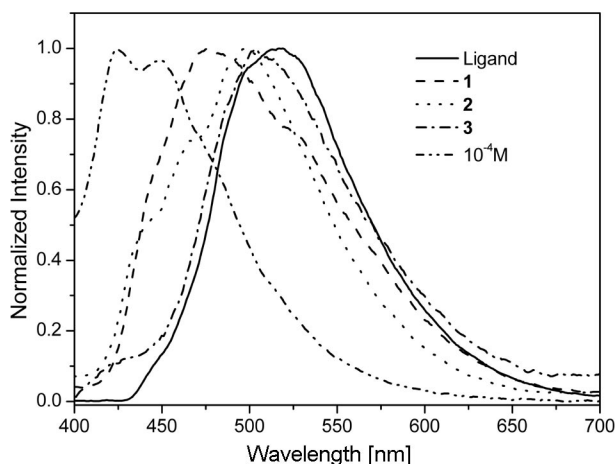
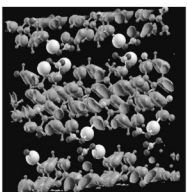
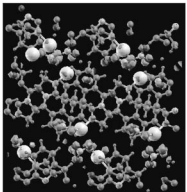
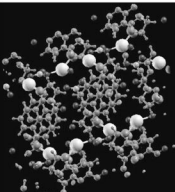
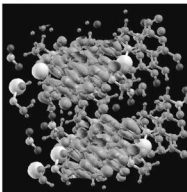
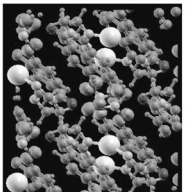
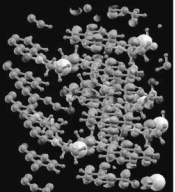
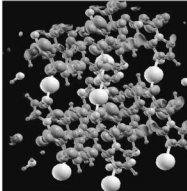
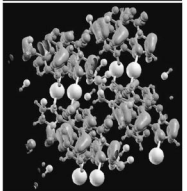
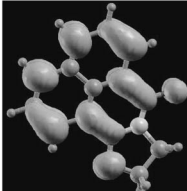
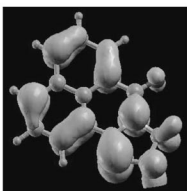


Figure 4. Emission spectra of **1–3** in the solid state, as well as the emission spectra of the free ligand in the solid state and in CH₂Cl₂ solution (10^{−4} M) at room temperature.

To explain the emission properties, periodical density function theory (SIESTA 2.0.2) was applied in the current case.^[22] The X-ray data was used to mimic the real situation in the solid state. A ligand was placed at the centre of a 50 Å cube to simulate the situation in the liquid state. Table 3 indicates that the HOMO and LUMO of the monomer and **3** are located mainly at the ligand. The electron distribution of the ligand supports our view that the excitation is mainly from ligand to ligand and that it has no interaction with the Ag atom.

Table 3 indicates the distributions of molecular orbitals (LUMO, HOMO, HOMO-2) of **1–3**. The LUMO primarily resides on the ligand. Complexes **1** and **2** have similar HOMO distributions. The HOMO and HOMO-1 are mainly located at the nitrate radical, and the HOMO-2 is mainly located at the ligand, while the HOMO resides on the ligand for **3**. Therefore, the excited states of **1–3** can be

Table 3. HOMO and LUMO distributions of complexes **1**, **2**, **3** and the ligand calculated by DFT methods.

	LUMO	HOMO	HOMO-2
1			
2			
3			
L			

assigned to LLCT transitions. The calculated energy gaps are listed in Table 4, and the data correspond to the emissive bands.

Table 4. HOMO and LUMO energies of complexes **1**, **2**, **3** and the ligand calculated by DFT methods.

	LUMO [eV]	HOMO [eV]	HOMO-2 [eV]
1	-4.88730	-6.85157	-7.11300
2	-5.22495	-6.68577	-7.19427
3	-5.19362		-7.32151
L	-3.27270	-5.61328	

Furthermore, the LUMO of every molecule, the HOMO of **3** and the HOMO-2 of **1** and **2** have no interaction with the Ag atom, and this could be explained by frontier molecular orbital theory.^[23] So, Ag atoms have no evident influence on the result, according to the experiments.

Conclusions

Three silver(I) complexes with 9,10-dihydro-7*H*-benzo[*de*]imidazo[2,1-*a*]isoquinolin-7-one have been synthesized and structurally characterized. The different conformations were obtained by the use of different counteranions or different ligand/Ag^I ion ratios. The π - π stacking interactions play an important role in the formation of these coordination polymers. Additionally, hydrogen bonding is also an indispensable element to construct supramolecular net-

works. Furthermore, complexes **1–3** display a blueshift in their emission with respect to that of the free ligand in the solid state at room temperature, and the luminescence of the silver(I) complexes mainly originates from ligand-centred π - π^* transitions.

Experimental Section

Materials and General Methods: All materials were commercially available and used without further purification. Elemental analyses of C, H and N were carried out with a Perkin–Elmer 2400 analyzer. FTIR spectra were obtained with a Nicolet Avatar 370 DTGS spectrometer with KBr pellets in the range 4000–400 cm⁻¹. ¹H NMR spectroscopic data were collected by using a Varian 300 MHz spectrometer. Chemical shifts were reported relative to TMS. Thermal stability (TG-DTA) studies were performed with a DTG-60H (Shimadzu) thermal analyzer from room temperature to 800 °C with a heating rate of 10 °C/min. Solid-state emission spectra of compounds were measured with a VARIAN CRAY 500 fluorescence spectrophotometer. Melting points were obtained with a XT4 Microscopic Melting-Point Detector (Beijing Keyi Electro-optic Instrument Plant).

[Ag(L)(NO₃)₂] (1): A solution of AgNO₃ (169 mg, 1 mmol) in methanol (10 mL) was added to a chloroform (10 mL) solution of **L** (216 mg, 1 mmol). The resulting solution was treated with nitric acid (5%) until pH \approx 6 and then stirred for 30 min at room temperature. After filtration, the clear solution was kept for many days at room temperature. Colourless crystals of **1** were collected with approximately 75% yield. C₂₈H₂₀Ag₂N₆O₈ (784.24): calcd. C 42.88, H 2.57, N 10.72; found C 42.69, H 2.48, N 10.88. FTIR (KBr pellets): $\tilde{\nu}$ = 3515 (m), 3439 (m), 3023 (m), 2973 (m), 2902 (m), 1698 (s), 1634 (s), 1595 (s), 1516 (m), 1494 (m), 1381 (s), 1315 (s), 1280 (s), 1120 (w), 1037 (w), 893 (w), 847 (w), 827 (w), 780 (s), 711 (w), 536 (m) cm⁻¹.

[Ag(L)₂(NO₃)] (2): Colourless crystals of **2** suitable for X-ray analysis were obtained by a procedure similar to that described for **1**, except for the ratio of the ligand and AgNO₃ (2:1 instead of 1:1). Yield: 80%. C₂₈H₂₀AgN₅O₅ (614.36): calcd. C 54.74, H 3.28, N 11.40; found C 54.32, H 3.35, N 11.86. FTIR (KBr pellets): $\tilde{\nu}$ = 3498 (s), 3358 (s), 3053 (s), 2970 (m), 2872 (w), 1659 (s), 1596 (s), 1482 (w), 1443 (w), 1384 (s), 1280 (s), 1233 (m), 1010 (m), 894 (w), 841 (m), 774 (s), 700 (w), 539 (m) cm⁻¹.

[Ag(L)₂](BF₄) (3): Colourless crystals of **3** suitable for X-ray analysis were obtained by a procedure similar to that described for **1**, except for using AgBF₄ instead of AgNO₃ and using fluoroboric acid instead of nitric acid to adjust pH value. Yield: 80%. C₂₈H₂₀AgBF₄N₄O₂ (639.16): calcd. C 54.74, H 3.28, N 11.40; found C 54.32, H 3.35, N 11.86. FTIR (KBr pellets): $\tilde{\nu}$ = 3514 (m), 3438 (m), 3027 (w), 2970 (m), 2901 (m), 1698 (s), 1634 (s), 1594 (s), 1514 (w), 1493 (w), 1376 (m), 1314 (m), 1280 (m), 1217 (w), 1111 (m), 1055 (s), 959 (w), 893 (w), 846 (w), 780 (s), 536 (m) cm⁻¹.

X-ray Crystallography: Single crystals of **1–3** were mounted on a Bruker Smart 1000 CCD diffractometer at 293 K equipped with Mo-*K*_α radiation (λ = 0.71073 Å). Absorption corrections were performed by using the SADABS program.^[24] All the structures were solved by direct methods and refined by full-matrix least-squares fitting on *F*² by SHELXL.^[25] All of the non-hydrogen atoms were refined anisotropically. Hydrogen atoms attached to C were located at geometrically calculated positions and refined with isotropic thermal parameters. For **3**, the tetrafluoroborate anions have disorder, the B atoms are in a special position, and the occupancy fac-

tors for B1, F1 and F1' atoms are all 0.50, while F^2 and $F^{2'}$ atom occupancy factors are 0.60 and 0.40, respectively. The crystallographic data are provided in Table 5. Selected bond lengths and angles are listed in Tables 1 and 2.

Table 5. Crystallographic data and structure refinement summary for **1–3**.

Complex	1	2	3
Chemical formula	$C_{28}H_{20}Ag_2N_6O_8$	$C_{28}H_{20}AgN_5O_5$	$C_{28}H_{20}AgBF_4N_4O_2$
Formula weight	784.24	614.36	639.16
T [K]	298(2)	298(2)	298(2)
Space group	$P2_1/n$	$P\bar{1}$	$P\bar{1}$
a [Å]	7.1454(9)	7.7991(9)	7.503(1)
b [Å]	21.404(3)	9.186(1)	9.124(2)
c [Å]	9.305(1)	18.013(2)	9.301(2)
α [°]	90	86.575(2)	87.511(3)
β [°]	112.074(2)	88.329(2)	70.495(3)
γ [°]	90	66.194(2)	88.295(3)
V [Å ³]	1318.8(3)	1178.5(2)	599.5(2)
Z	2	2	1
D_{calcd} [Mg/m ³]	1.975	1.731	1.770
μ [mm ⁻¹]	1.552	0.909	0.909
Data/parameters	2864/199	4995/352	2532/192
R_1	0.0770	0.0857	0.0517
wR_2	0.1690	0.1024	0.1325

CCDC-701804 (for **1**), CCDC-701805 (for **2**) and CCDC-701806 (for **3**) contain the supplementary crystallographic data for this paper. These data can be obtained free of charge from The Cambridge Crystallographic Data Centre via www.ccdc.cam.ac.uk/data_request/cif.

Computational Details: The simulation was run under SIESTA 2.0.2 with numerical-orbital basis sets. GGA-PBE was used for The exchange-correlation function. The standard basis set was used. The Meshcutoff was 150 Ry and orbital-confining cutoff radii were determined from an energy shift of 0.01. To simulate the solid situation effectively, we have widely used X-ray data to mimic the real situation. Because of the difference between reality and simulation, variablecell was set true. The parallel diagonalization method was used to speed up calculations. The accuracy was carefully benchmarked with the plane-wave code previously.

Supporting Information (see footnote on the first page of this article): TGA for **1**, **2**, **3**.

Acknowledgments

The authors thank Prof. Xiao-Ming Chen (Sun Yat-Sen University) for his help in the revision of paper. This work was financially supported by the National Natural Science Foundation of China (50802059), Shanghai Municipal Education Commission (09YZ159, 07ZZ68), the Key Project from the Science and Technology Foundation of Shanghai (065212050), the Shanghai Key Laboratory of the Rare Earth Functional Materials (07dz22303), the Shanghai Leading Academic Discipline Project (S30406), Shanghai for Key Topics in Innovation Engineering (Inorganic Chemistry) and Shanghai Normal University (PL814).

- [1] a) C. L. Chen, B. S. Kang, C. Y. Su, *Aust. J. Chem.* **2006**, *59*, 3–18; b) L. M. Chiang, C. W. Yeh, Z. K. Chan, K. M. Wang, Y. C. Chou, J. D. Chen, J. C. Wang, J. Y. Lai, *Cryst. Growth Des.* **2008**, *8*, 470–477; c) A. G. Young, L. R. Hanton, *Coord. Chem. Rev.* **2008**, *252*, 1346–1386; d) S. Hiraoka, T. Yi, M. Shiro, M. Shionoya, *J. Am. Chem. Soc.* **2002**, *124*, 14510–

- 14511; e) E. D. Genuis, J. A. Kelly, M. Patel, R. McDonald, M. J. Ferguson, G. Greidanus-Strom, *Inorg. Chem.* **2008**, *47*, 6184–6194; f) M. Morgan, J. Rebek Jr, *Chem. Rev.* **1997**, *97*, 1647–1668.
- [2] A. Barbieri, G. Accorsi, N. Armaroli, *Chem. Commun.* **2008**, 2185–2193 and references therein.
- [3] L. Carlucci, G. Ciani, D. W. v. Gudenberg, D. M. Proserpio, *Inorg. Chem.* **1997**, *36*, 3812–3813.
- [4] a) A. Bellusci, A. Crispini, D. Pucci, E. I. Szerb, M. Ghedini, *Cryst. Growth Des.* **2008**, *8*, 3114–3122; b) G. K. Patra, I. Goldberg, S. De, D. Datta, *CrystEngComm* **2007**, *9*, 828–832; c) R. P. Feazell, C. R. Carson, K. K. Klausmeyer, *Inorg. Chem.* **2006**, *45*, 2627–2634; d) R. P. Feazell, C. R. Carson, K. K. Klausmeyer, *Inorg. Chem.* **2006**, *45*, 2635–2643.
- [5] A. J. Blake, N. R. Champness, P. A. Cooke, J. E. B. Nicolson, *Chem. Commun.* **2000**, 665–666.
- [6] a) R. P. Feazell, C. R. Carson, K. K. Klausmeyer, *Eur. J. Inorg. Chem. Eur. J. Inorg.* **2005**, 3287–3297; b) X.-H. Bu, W. Chen, W.-F. Hou, M. Du, R.-H. Zhang, F. Brisse, *Inorg. Chem.* **2002**, *41*, 3477–3482; c) A. J. Blake, N. R. Champness, P. A. Cooke, J. E. B. Nicolson, C. Wilson, *J. Chem. Soc., Dalton Trans.* **2000**, 3811–3819.
- [7] a) J. Dinda, S. Jasimuddin, G. Mostafa, C.-H. Hung, C. Sinha, *Polyhedron* **2004**, *23*, 793–800; b) C. Fan, C.-B. Ma, C.-N. Chen, F. Chen, Q.-T. Liu, *Inorg. Chem. Commun.* **2003**, *6*, 491–494; c) A. Melaiye, Z. H. Sun, K. Hindi, A. Milsted, D. Ely, D. H. Reneker, C. A. Tessier, W. J. Youngs, *J. Am. Chem. Soc.* **2005**, *127*, 2285–2291; d) T. Ramnial, C. D. Abernethy, M. D. Spicer, I. D. McKenzie, I. D. Gay, J. A. C. Clyburne, *Inorg. Chem.* **2003**, *42*, 1391–1393; e) H. F. Zhu, J. Fan, T. Okamura, W. Y. Sun, N. Ueyama, *Cryst. Growth Des.* **2005**, *5*, 289–294.
- [8] a) H.-Y. Tan, H.-X. Zhang, H.-D. Ou, K.-B. Sang, *Inorg. Chim. Acta* **2004**, *357*, 869–874; b) J. Fan, W.-Y. Sun, T. Okamura, W.-X. Tang, N. Ueyama, *Inorg. Chim. Acta* **2004**, *357*, 2385–2389; c) M. A. Jalil, T. Yamada, S. Fujinami, T. Honjo, H. Nishikawa, *Polyhedron* **2001**, *20*, 627–633; d) F. Bachechi, A. Burini, R. Galassi, B. R. Pietroni, M. Ricciutelli, *Inorg. Chim. Acta* **2004**, *357*, 4349–4357; e) J.-W. Wang, H.-B. Song, Q.-S. Li, F.-B. Xu, Z.-Z. Zhang, *Inorg. Chim. Acta* **2005**, *358*, 3653–3658; f) R. Rowan, R. Tallon, A. M. Sheahan, R. Curran, M. McCann, K. Kavanagh, M. Devereux, V. McKee, *Polyhedron* **2006**, *25*, 1771–1778; g) L.-X. Xie, M. Xie, C.-Y. Duan, Q.-Z. Sun, Q.-J. Meng, *Inorg. Chim. Acta* **2007**, *360*, 2541–2548; h) C. Ganesamoorthy, M. S. Balakrishna, J. T. Mague, H. M. Tuononen, *Inorg. Chem.* **2008**, *47*, 2764–2776.
- [9] a) S.-P. Yang, H.-L. Zhu, X.-H. Yin, X.-M. Chen, L.-N. Ji, *Polyhedron* **2000**, *19*, 2237–2242; b) B. Zhao, X.-Q. Zhao, W. Shi, P. Cheng, *J. Mol. Struct.* **2007**, *830*, 143–146; c) A. Beheshti, W. Clegg, N. R. Brooks, F. Sharafi, *Polyhedron* **2005**, *24*, 435–441.
- [10] a) J.-M. Chen, J.-J. Sun, W.-W. Huang, Y.-N. Lao, S.-P. Yang, *Acta Crystallogr., Sect. E* **2006**, *62*, m2573–m2574; b) S.-P. Yang, H.-M. Chen, F. Zhang, H.-M. Chen, *Appl. Organomet. Chem.* **2004**, *18*, 88–89; c) S.-P. Yang, X.-M. Chen, L.-N. Ji, *J. Chem. Soc., Dalton Trans.* **2000**, 2337–2344; d) L.-S. Long, S.-P. Yang, T.-X. Tong, Z.-W. Mao, X.-M. Chen, L.-N. Ji, *J. Chem. Soc., Dalton Trans.* **1999**, 1999–2004; e) S.-P. Yang, L.-S. Long, X.-M. Chen, L.-N. Ji, *Acta Crystallogr., Sect. C* **1999**, *55*, 869–871; f) S.-P. Yang, Y.-X. Tong, H.-L. Zhu, H. Cao, X.-M. Chen, L.-N. Ji, *Polyhedron* **2001**, *20*, 223–229.
- [11] E. Martín, J. L. G. Coronado, J. J. Camacho, A. Pardo, *J. Photochem. Photobiol. A: Chem.* **2005**, *175*, 1–7.
- [12] a) I. Grabchev, C. Petkov, V. Bojinov, *Dyes Pigm.* **2001**, *48*, 239–244; b) X. Qian, K. Zhu, K. Chen, *Dyes Pigm.* **1989**, *11*, 13–20.
- [13] a) W. W. Stewart, *Nature* **1981**, *292*, 17–21; b) A. Pardo, E. Martín, J. M. L. Poyato, J. J. Camacho, J. M. Guerra, R. Weigand, J. M. F. Braña, J. M. Castellano, *J. Photochem. Photobiol. A: Chem.* **1989**, *48*, 259–263; c) E. Martín, R. Weigand, A. Pardo, *J. Lumin.* **1996**, *68*, 157–164.

- [14] a) C.-X. Xia, B.-H. Ye, F. He, L. Cheng, X.-M. Chen, *CrytEngComm* **2004**, *6*, 200–206; b) T.-B. Huang, J.-F. Zhang, D.-H. Zhu, W. Yao, X.-H. Qian, *Synthesis* **1999**, *7*, 1109–1111.
- [15] ^1H NMR (300 MHz, CDCl_3): δ = 4.2 (b, 4 H, $-\text{CH}_2$), 7.7 (t, 2 H, C_{10}H_6), 8.1 (d, 2 H, C_{10}H_6), 8.5 (s, 2 H, C_{10}H_6) ppm. FTIR (KBr pellets): $\tilde{\nu}$ = 3498 (m), 3357 (s), 3057 (w), 3014 (w), 2962 (m), 2934 (w), 1665 (s), 1615 (s), 1590 (s), 1504 (w), 1463 (s), 1443 (m), 1413 (s), 1344 (s), 1279 (s), 1230 (s), 1118 (w), 1007 (s), 894 (m), 838 (m), 768 (s), 538 (s) cm^{-1} .
- [16] X.-P. Li, J.-Y. Zhang, M. Pan, S.-R. Zheng, Y. Liu, C.-Y. Su, *Inorg. Chem.* **2007**, *46*, 4617–4625.
- [17] M.-L. Tong, X.-M. Chen, S.-W. Ng, *Inorg. Chem. Commun.* **2000**, *3*, 436–441.
- [18] M. Jansen, *Angew. Chem. Int. Ed. Engl.* **1987**, *26*, 1098–1110.
- [19] V. T. Yilmaz, S. Hamamci, S. Gumus, *Chem. Phys. Lett.* **2006**, *425*, 361–366.
- [20] N. J. Turro, *Modern Molecular Photochemistry*, University Science Books, Sausalito, CA, **1991**.
- [21] a) Y. P. Tong, S. L. Zheng, X. M. Chen, *Inorg. Chem.* **2005**, *44*, 4270–4275; b) Y. P. Tong, S. L. Zheng, X. M. Chen, *Eur. J. Inorg. Chem.* **2005**, 3734–3741.
- [22] a) J. M. Soler, E. Artacho, J. D. Gale, A. Garcia, J. Junquera, P. Ordejon, S. Portal, *J. Phys.: Condens. Matter* **2002**, *14*, 2745–2779; b) Z. P. Liu, X. Q. Gong, J. Kohanoff, C. Sanchez, P. Hu, *Phys. Rev. Lett.* **2003**, *91*, 266102; c) S. L. Zheng, X. M. Chen, *Aust. J. Chem.* **2004**, *57*, 703–712 and references cited therein.
- [23] I. Fleming, *Frontier Orbitals and Organic Chemical Reactions*, John Wiley & Sons, New York, **1976**.
- [24] a) *Smart NT Smart*. Version 5.0, Bruker Industrial Automation Inc., Madison, WI, **1998**; b) Bruker (1998). SMART, SADABS (Version 5).
- [25] a) G. M. Sheldrick, *SHELXS-97, Program for X-ray Crystal Structure Solution*, University of Göttingen, Germany, **1997**; b) G. M. Sheldrick, *SHELXS-97, Program for X-ray Crystal Structure Refinement*, University of Göttingen, Germany, **1997**.

Received: March 13, 2009

Published Online: May 18, 2009